J Fluoresc (2011) 21:1053–1060
DOI 10.1007/s10895-010-0777-z

ORIGINAL PAPER

Enhanced Green Emission from Er_2WO_6 Nanocrystals Embedded Composite Tellurite Glasses

Sathravada Balaji · Dipten Misra · Radhaballabh Debnath

Received: 18 September 2010 / Accepted: 16 November 2010 / Published online: 8 December 2010

Abstract A series of tungsten-tellurite glasses activated with different concentrations (0–1.5 mol %) of Er^{3+} has been synthesized. The structural properties of the best luminescent sample and the optical properties of its Er^{3+} ions, are studied both immediate after its preparation as well as after its ageing. On ageing the glass suffers structural reorganization and generates Er_2WO_6—nanocrystals in the matrix, which greatly enhances the normal and upconversion green luminescence efficiency of Er^{3+}. The nanocrystal aided enhancement of normal and upconversion luminescence of Er^{3+} of the glass has been attributed to the crystal field effects of the new environment of Er^{3+} in the nanocrystals. A phenomenon of preferential enhancement of red upconversion luminescence at the cost of green upconversion luminescence of Er^{3+} at its higher concentrations in the glass has been observed and the related photo-physics is proposed. The material shows the prospect of being used as NIR solar concentrator.

Keywords $Er^{3+} \cdot Er_2WO_6$ nanocrystals · Luminescence · Upconversion

S. Balaji
Central Glass and Ceramic Research Institute (CGCRI),
Council of Scientific and Industrial Research (CSIR),
196, Raja S. C. Mullick Road,
Kolkata 700 032, India
e-mail: sbalaji@cgcri.res.in

D. Misra · R. Debnath (✉)
School of Laser Science and Engineering, Jadavpur University,
Jadavpur,
Kolkata 700 032, India
e-mail: debnathr@hotmail.com

D. Misra
e-mail: dipten@gmail.com

Introduction

Rare earth ions activated crystals and glasses, are technologically important [1–16] because of their applications in different optics and optoelectronics, like solid state lasers [1–4], anti-Stokes luminescence cooling [5], optical communications [1–4], energy up conversion [6–12, 15] etc. Light energy upconversion property of such materials has particularly received interest in the recent years because of their prospective use in biological labeling [9, 10] and solar NIR concentration for photovoltaic exploitation [14]. As far as the application as solar NIR concentrator, is concerned, big panels either wholly made up of upconverting materials or monolithic panels dispersed with upconverting nanocrystals [16] are preferred. In that respect, nanocrystals dispersed upconverting glasses seem to be the ideal candidates both in terms of efficiency and large area coverage.

In our previous studies [15, 16] we reported results of our theoretical and experimental investigations on the optical properties of some Er-related nanocrystals dispersed tellurite glasses and predicted that they might be promising for use as solar NIR concentrator and medium for upconversion laser.

In the present paper, we report upconversion luminescence properties of Er_2WO_6—nanocrystals dispersed tungsten tellurite glasses. It has been observed that after the growth of Er_2WO_6—nanocrystals in the glass intensities of both the normal and upconversion luminescence of Er^{3+} are remarkably enhanced. Studies on the effect of the variation of Er^{3+} concentration on the upconversion luminescence showed that at higher concentrations Er^{3+} the red upconversion luminescence ($^4F_{9/2} \rightarrow {}^4I_{15/2}$) of the glass get preferentially enhanced at the cost of upconversion green luminescence. The photo-physics of all such effects have been discussed.

Materials and Sample Preparation

(W, La)-tellurite glasses of composition (mol %): (80 to 90) TeO_2, [(10 to 5)–x]BaO, 2x[PbF_2 + WO_3], (5–y)La_2O_3, yEr_2O_3, $0 < y < x \leq 5$, with different concentration of Er^{3+} (up to 1.5 mol %) were melted at 700–750 °C for two hours in an electric furnace using platinum crucible. All the chemicals used were of AR grade (Sigma-Aldrich). The molten glass in each case was cast and then annealed for 12 h at 300 °C in an annealing furnace. Initial measurement with the samples showed that the luminescence efficiency of the sample containing 1 mol % of Er_2O_3 was the highest. So the sample containing 1 mol % of Er_2O_3 was chosen for most of the present studies. Only the study on the effect of variation of Er^{3+} concentration on its luminescence efficiency, were carried out using samples of different concentration of Er_2O_3. The Er_2WO_6 nanocrystals in the glass were grown by ageing the glass under ambient condition. The crystallization was found to reach to almost completion by a month or so. To see the effect of crystallization on different optical properties of the glass, studies were made both at the freshly prepared and the aged stage of the glass.

Measurement Techniques

All absorption and reflectance spectra were recorded at 300 K in an UV-VIS-NIR absorption spectrophotometer (Shimadzu, Japan, model: 3001). A plate-shaped polished sample (average thickness d = 1.15 ± 0.01 mm) of the glass was used for absorption study. A similar plate of the base glass of average thickness d ~ 1.15 ± 0.01 mm was used as the reference to obtain the base glass corrected absorption spectrum. Density of the glass was measured by Archimedes method (D = 5.36 ± .005 g/cm^3). Concentration of Er^{3+} in the glass was found to be ~3.67 × 10^{20} ions /cm^3.

The X-ray powder diffraction spectra of the freshly prepared as well as the aged glass were recorded in an X-ray diffract meter (model: PW1710 BASED, make: Philips) using a copper anode. A Field Emission Scanning Electron Microscope (FESEM, Supra-35 VP, make: Carlzeiss SMT, Germany) was used to record the micrographs of the samples. The SAED of nanocrystals in the glass was recorded in a 200 KV HRTEM, model: JEM-2011, make: JEOL, Japan.

The emission spectra of the glasses were recorded in a Perkin Elmer LS55 Spectrofluorimeter. Quantitative study of the emission of the glass, at its freshly prepared stage as well as after its ageing, was made by using 'front surface luminescence' technique and keeping the sample-position, emission and excitation slits and the lamp-voltage, unaltered. The quantitative upconversion luminescence spectra under different power of the laser-excitation, were recorded in the same spectrofluorimeter by using a fiber pig-tailed 976 nm diode laser (Thor Lab, USA) with variable output power and fixing the sample in a sample holder at a definite distance from the tip of the laser output fiber. Other parameters were maintained similar to those described before. The upconversion luminescence of the glass, at its freshly prepared stage, was too weak to record by our experimental set up.

The excited state dynamics of the $^4S_{3/2}$ luminescent state of Er^{3+} in the freshly prepared as well as aged glass were studied in a luminescence lifetime measurement setup (Fluorocube, IBH, UK) by using multichannel analyzer technique. A Spectra-LED of 372 nm with pulse duration of 100 μs and repetition rate of 100 Hz, was used as excitation source. To avoid any mixing of the excitation-pulse profile with the sample's decay, only the data of the photon-channels lying beyond the excitation pulse duration were considered.

Experimental Results

Absorption and Reflectance Spectra

Figure 1 shows the base-glass corrected absorption spectrum of Er^{3+} ions in the glass along with that of the base glass which has a strong UV-absorption edge right from ~400 nm. The spectrum exhibits a number of distinct absorption bands of Er^{3+} around 489, 522, 545, 653, 800, 977 and 1533 nm. The bands can be easily assigned [4, 13, 16] as the electronic transitions of Er^{3+} from its ground $^4I_{15/2}$ state to the $^4F_{7/2}$,

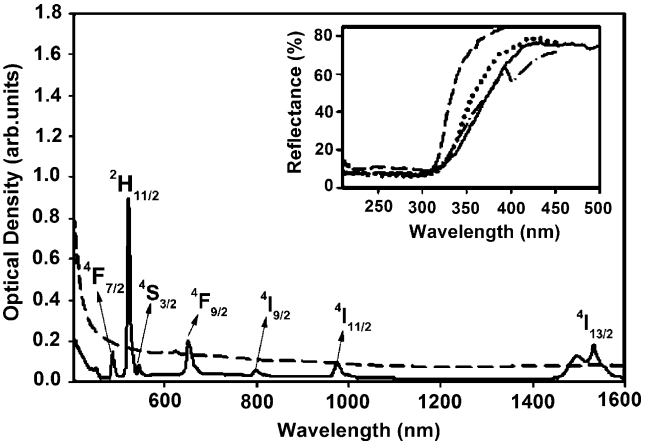

Fig. 1 Absorption spectrum of the base glass (- - - - -); base glass corrected absorption spectrum of Er^{3+} in the tungstate- tellurite glass (___); [sample thickness (d) in both the cases ~1.15 ± 0.01 mm]. **Inset:** Reflectance spectra: The base glass (-.-.-.); a glass similar in composition but devoid of WO_3 (……); the nanocrystals bearing glass (___); TeO_2 (- - - - -); [spectra are not normalized]

$^2H_{11/2}$, $^4S_{3/2}$, $^4F_{9/2}$, $^4I_{9/2}$, $^4I_{11/2}$ and $^4I_{13/2}$ excited states respectively. Because of the onset of the strong UV-absorption edge of the base glass from ~400 nm, the $^4I_{15/2}\rightarrow{}^2G_{9/2}$ and $^4I_{15/2}\rightarrow{}^4G_{11/2}$ transitions of Er^{3+} are not visible in the spectrum.

The inset of Fig. 1 shows the reflectance spectrum of the powdered base glass along with that of the aged Er^{3+} activated glass. The similar reflectance spectra of TeO_2, and a glass of similar in composition but devoid of WO_3 and Er^{3+} ions, are also shown side by side. Neither the tellurium oxide which is the major component of the present glass, nor the glass which is devoid of tungsten and Er^{3+}, has significant absorption in the visible region beyond 350 nm. Addition of WO_3 in the composition, however, causes additional absorption covering the region 350–400 nm (a shoulder around 360 nm and distinct peak at 390 nm). Network of a tungstate–tellurite glass is known [17] to consists of two types of tellurite units and one type of tungstate unit (O = WO_5 octahedron). It is also reported in literature [18, 19] that such tungsten oxide shows a broad absorption band around 390 nm, suggesting a correspondence with the feature observed in the reflectance spectrum of the base glass at the same wavelength (see inset of Fig. 1). Surprisingly the reflectance spectrum of the aged Er^{3+}- activated glass does not show any feature at ~390 nm. The result suggests that in presence of Er^{3+}, the tungstate units (O = WO_5) of the glass possibly suffers some slow reorganization in its structure to form a new phase with different absorption feature.

Micro and Nanoscopic Structure of the Glass

FESEM picture of the aged glass (Fig. 2) shows existence of nanoclusters of sizes ranging approximately, from 20 to 80 nm in the glass matrix. The inset of Fig. 2 shows the magnified image of a single cluster which contains many nanocrystals of sizes ranging from 5 to 8 nm. To see whether the freshly prepared glass also contains such nanocrystals and to understand about its phase, X-ray powder diffraction spectra, of both the freshly prepared and the aged glass samples were recorded. Because the crystallite sizes of the nanocrystals were very small (5–8 nm) and the major part of the system was in the glassy phase, we could not get well defined diffraction peaks in XRD spectra in the cases of both the samples. Such spectra are shown in the Fig. 3 and its inset. The spectra of both the samples exhibit a relatively sharp band peaking around $2\theta \sim 30^o$ ($d \sim 3.11A^o$) along with a broad halo. The presence of a sharp band in each spectrum has indicated that there is definitely a phase in each glass which is crystalline. A comparative study of the two spectra however shows that the sharp band in the case of the freshly prepared sample is almost 6–7 times less intense than that of the aged sample. It is also revealed that the freshly prepared glass attains crystallization only about ~15–16 % of the fully crystallized stage. Further scrutiny of the spectrum of the aged sample (Inset of Fig. 3), shows that the sharp band, is in fact, asymmetric in nature and exhibits feature of mixing of at least two lines one around d ~ 3.11A° and the other with almost equal intensity at around d ~ 3.01A°. The noisy character of the spectrum however did not allow us to identify any other diffraction lines in the spectrum. In an attempt to get further information about the nature of the phase of the nanocrystals, we have recorded SAED of the nanocrystallites of the aged sample. This is shown in Fig. 4. The SAED pattern shows one distinct Scherrer ring at d ~ 1.81A°, and one blurred ring in between d = 3.11–3.00A°. Observation of the blurred Scherrer ring in between d = 3.11–3.00A° in the SAED, seems to corroborate our previous detection of two closely spaced lines at d ~ 3.11A° and ~3.01A° in the XRD spectrum of the aged sample. In fact, the Scherrer-rings, corresponding to two closely spaced

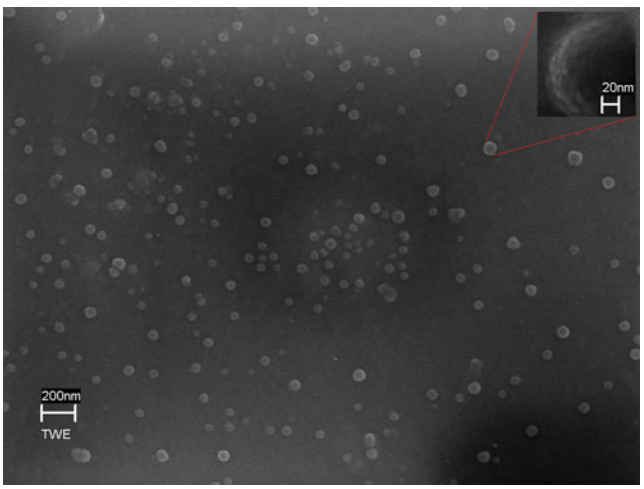

Fig. 2 FESEM picture of the Er^{3+} doped aged tungstate- tellurite glass. **Inset:** Magnified Image

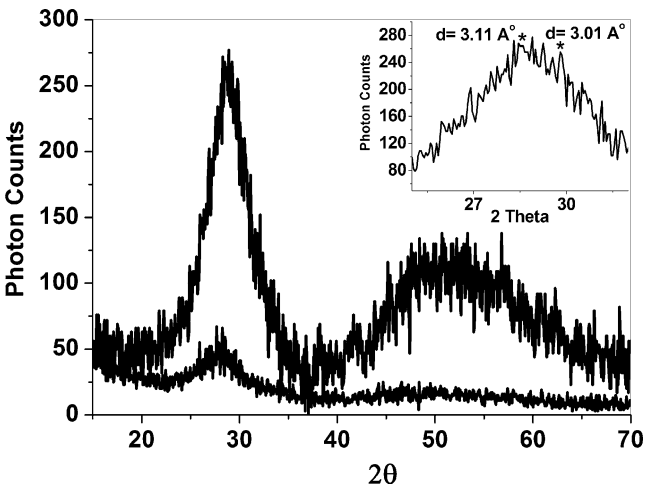

Fig. 3 XRD spectrum of the freshly prepared Er^{3+} doped glass and the aged glass. **Inset:** Expanded version of the relatively sharp peak

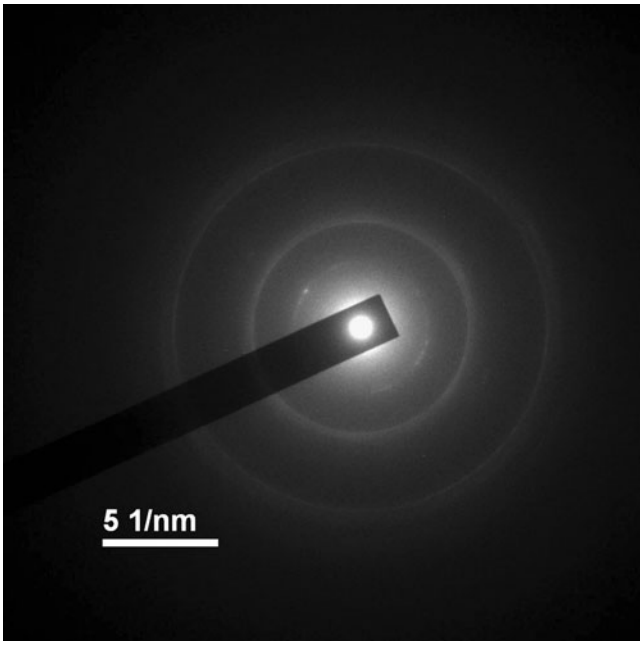

Fig. 4 SAED spectrum of the nanocrystals of the glass showing Scherrer rings

lattice planes, are expected to overlap each other making the ring smeared rather than distinct. Now consideration of the chemical composition of the glass, suggests that the possible crystalline phases which may grow in such glass, are PbF_2, tungstates or/and tellurates respectively of the types $M_2[WO_6]$ and $M_2Te_4O_{11}$ (where M = Er^{3+}, La^{3+}). The glass was prepared by melting at 700–750 °C for 2 h, so the possibility of presence of sufficient fluorine in the glass to form a fluoride phase seems to be remote. Scrutiny of XRD–data files of the above mentioned phases also suggests that the detected three diffraction lines [d ~ 3.11A° (I = 100), ~3.01A° (I ~ 100) and ~1.81A°] of the nanocrystalline phase closely match with the main diffraction lines of (Er_2WO_6) [20–22]. Tyulin et al however, reported [21, 22] very closely spaced three high intensity lines [one at d = 3.08A° (I = 100, hkl = −2–11) and two other lines around d = 3.01A° of respective hkl = −11–3 and 013] for (Er_2WO_6). Our XRD spectrum could not show the further resolution of the line at d ~ 3.01A° because of its noisy character. We however, have confirmed the identity of the nanocrystalline phase as (Er_2WO_6) from the calculated values of Judd–Ofelt parameters as well as the life-time measurement data of the $^4S_{3/2}$ emitting state of Er^{3+} which will be discussed in the following sections.

Nanocrystals and Enhancement of Luminescence Efficiency and Life-Time of the $^4S_{3/2}$ State of Er^{3+}

In spite of the fact that the base glass itself has a very strong UV absorption edge starting from ~400 nm, the aged glass upon excitation in the wavelength region of 350–400 nm, exhibits a strong green luminescence peaking around 535 and 548 nm due to ($^2H_{11/2}$, $^4S_{3/2}$)→$^4I_{15/2}$ transitions of Er^{3+}. Figure 5 shows such luminescence spectrum of the aged sample under 380 nm excitation vis-à-vis that of the freshly prepared glass. An estimate of the ratio of the integrated emissions (IE) of the two cases (IE_{aged}/IE_{fresh} = 20,450/3,149 = 6.5), shows that the luminescence efficiency of the glass is enhanced more than six times after complete growth of $Er_2[WO_6]$ nanocrystals in the matrix. In addition to the enhancement of luminescence a significant change in the spectral resolution (e.g. clear appearance of the Stark split components) as well as a reversal in the peak intensities, are also noted. The results show that the Er^{3+} ions in the aged glass experience a stronger and regular crystal field after the growth of the nanocrystals. Before the growth of nanocrystals, the Er^{3+} ions remain randomly dispersed in the interstitial of the network structure of the glass. After the formation of the $Er_2[WO_6]$ nanocrystals, Er^{3+} ions of the nanocrystals achieve a well defined surrounding and hence experience a well defined crystal field. We reported [15] earlier that the Judd–Ofelt parameters and the calculated life time of the $^4S_{3/2}$→$^4I_{15/2}$ emission of Er^{3+} of the aged glass were [Ω_2–8.410 × 10^{-20} cm^2, Ω_4 = 4.833 × 10^{-20} cm^2 and Ω_6 = 2.027 × 10^{-20} cm^2] and 219.4 μs respectively. The high value of Ω_2 indicated that the crystal field surrounding the Er^{3+} ions in the aged glass was very strong. Wang et al [23] recently showed that incorporation of tungsten oxide in Eu^{3+} containing glass had pronounced effect on the surrounding field of Eu^{3+} ion and hence greatly influenced the value of its Ω_2. Similar phenomenon is expected in case of our aged glass also.

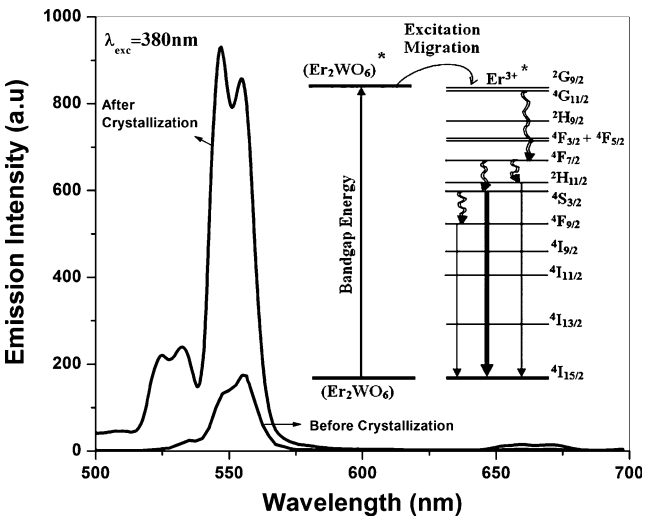

Fig. 5 Green and red luminescence of Er^{3+} ions in the freshly prepared and in the aged glass respectively. **Inset:** Mechanism of excitation migration from $Er_2[WO_6]$ nanocrystals to the Er^{3+} ions

The Fig. 6 and its Inset show the decay profile of the excited $^4S_{3/2}$ emitting state of Er^{3+} in the aged as well as in the freshly prepared glass respectively. In the case of the freshly prepared sample (Inset of Fig. 6), the decay shows a bi-exponential character (with a faster component of life time ~17 ± 1.044 μs and a relatively slower component of life time ~38 ± 2.524 μs). In the case of the aged sample (Fig. 6) the decay is also non-exponential and its best fit result indicates a tri-exponential character (a faster component of life time ~10 ± 1.145 μs and two slower components of life time ~56 ± 1.212 μs and ~157 ± 1.456 μs). The origin of the faster component observed in the cases of both the freshly prepared and the aged sample (~17 ± 1.044 μs and ~10 ± 1.145 μs) seems to be related to the excitation pulse. The slower component of the decay of the freshly prepared sample should mainly represent Er^{3+} ions of the glassy phase, because in this sample contribution from the crystalline phase should be small. In the case of aged sample, the two slower components of the decay (~56 ± 1.212 μs and ~157 ± 1.456 μs) therefore, represent the Er^{3+} ions lying respectively in the glassy and the nanocrystalline phases. A significant change in the life-time of the $^4S_{3/2}$ emitting state of a fraction of Er^{3+} ions [from ~(40–56) μs to 157 μs] after the growth of the nanocrystals, that Er^{3+} ions associated with the nanocrystals of the glass and the surrounding field of Er^{3+} in the nanocrystals is different from that of the ion in the glass where environment is mainly $(\text{-Te-O})_n$ type. Judd–Ofelt calculation also yielded [15] similar high value of the life time of ~219.4 μs. Thus the phase of the nanocrystals of the aged glass, must be the (Er_2WO_6) rather than ($Er_2Te_4O_{11}$). Had the phase been the ($Er_2Te_4O_{11}$), a drastic change in the excited state life-time of Er^{3+} was not expected, because such a phase would not create any new environment surrounding the Er^{3+} ions.

Nanocrystals and its Effect on the Upconversion Luminescence of Er^{3+}

As described in the experimental section that the quantitative upconversion luminescence spectra of the glass were recorded as a function of laser power, after exciting the Er^{3+} ions into its $^4I_{11/2}$ excited state using a 976 nm diode laser. In spite of our best effort we could not detect any upconversion luminescence of Er^{3+} in the case of freshly prepared sample. Interestingly, the aged glass (i.e. the $Er_2[WO_6]$-nanocrystals bearing glass) showed a very strong upconversion green luminescence peaking at 533 and 550 nm due to ($^2H_{11/2}$, $^4S_{3/2}$)→$^4I_{15/2}$ transitions along with a weak red emission at ~670 nm due to ($F_{9/2}$→$^4I_{15/2}$) transition of Er^{3+}. The upconversion spectra as a function of laser power are shown in Fig. 7. The result clearly shows that the growth of the $Er_2[WO_6]$-nanocrystals in the glass significantly enhances the upconversion luminescence of Er^{3+}.

In case of an upconversion luminescence, upconversion luminescence intensity I_{upc} is related to the intensity of the excitation source I_{exci} by the following relation: $I_{upc} \propto I_{exci}^{m}$, where 'm' is the number of photons (low energy) absorbed per visible photon emitted.

A plot of log I_{upc} vs log $I_{exci,}$ should therefore, give a straight line with a slope = m. The Inset of the Fig. 7 shows such plots for different upconversion emissions of

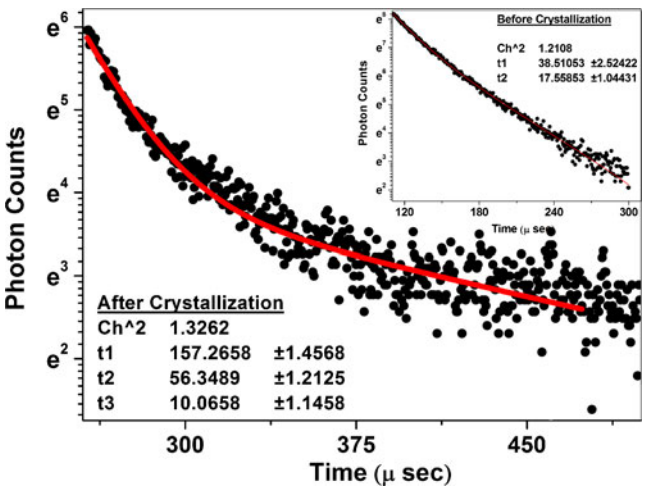

Fig. 6 Decay profile of the excited $^4S_{3/2}$ emitting state of Er^{3+} in the aged glass. **Inset:** Decay profile of the excited $^4S_{3/2}$ emitting state of Er^{3+} in the freshly prepared glass

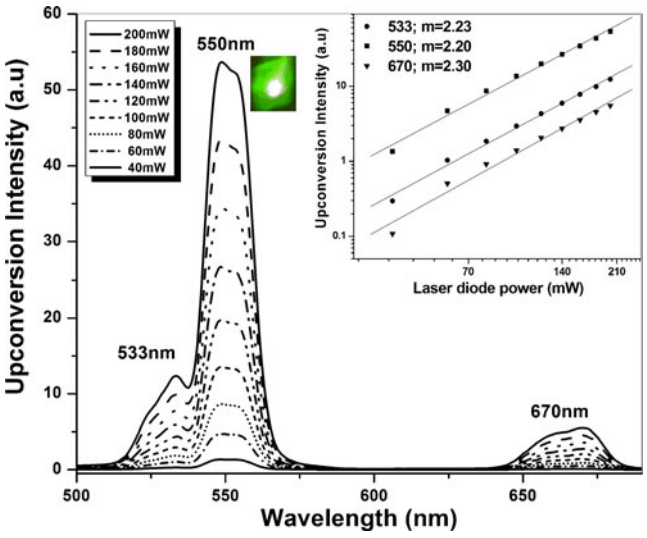

Fig. 7 Upconversion luminescence of Er^{3+} of the aged glass as a function of excitation power of the 976 nm laser. (Upconversion green emission picture under 200 mW). **Inset**: Logarithmic plot of the peak intensity vs. laser power

Er^{3+} in the $Er_2[WO_6]$—nanocrystals bearing glass. The values of 'm' obtained for 533, 550 and 670 nm emissions are 2.23, 2.20 and 2.30 respectively. The results indicate that all the upconversion emission processes are biphotonic in nature.

The Effect of Concentration of Er^{3+} on its Green and Red Upconversion Luminescence

The effect of variation of Er^{3+}—concentration (up to 1.5 mol%) on the green and red upconversion luminescence of the glasses has also been studied under excitation of 200 mW power of the 976 nm diode laser. These are shown in Fig. 8. It is clear from the plots that in the case of the green upconversion luminescence, intensity of the luminescence increases with the increase of concentration of Er^{3+} and maximizes around 1–1.1 mol % of Er_2O_3. But in case of the red upconversion luminescence the picture is different, a concentration of 1.5–1.6 mol % of Er_2O_3 is required to get an optimum intensity.

Discussions

The results of the observed enhancement of both the normal and upconversion luminescence efficiency of Er^{3+} in the case of the aged glass, suggest that the phenomenon should be related to the changed crystal field environment of Er^{3+} in the newly grown (Er_2WO_6)—nanocrystals. The new field possibly induces different intra-centre excitation rates and/or different non-radiative decay path to the ion.

The observed significant change in the excited state lifetime of the $^4S_{3/2}$ emitting state of Er^{3+} after the growth of nanocrystals also supports the above view. In the case of excitation of the aged glass through its near UV absorption edge region (350–400 nm), an additional effect like (Er_2WO_6)—band gap mediated excitation of Er^{3+} also takes place, which enhances the overall luminescence efficiency of the ion almost six times compared to that of the freshly prepared sample. Possible mechanism of such (Er_2WO_6)—band gap mediated excitation of Er^{3+} ions in the aged glass, is shown in the 'Inset' of Fig. 5. Now considering the case of upconversion luminescence of the aged glass, it is evident that the newly formed crystal field induces different intra-centre excitation rates, which cause more efficient excitation of Er^{3+} ions to the $^4I_{11/2}$ state when the glass is exposed to the 976 nm laser. A relatively long life time [12, 15] of the excited $^4I_{11/2}$ state suggests that only a fraction of the ions of the excited state relaxes to the immediate low lying $^4I_{13/2}$ state and the major fraction stays in the excited $^4I_{11/2}$ state for a reasonably long time. Such a phenomenon gives the ions of the $^4I_{11/2}$ excited state an opportunity to absorb a second photon through excited state absorption (ESA) and reach the $^2H_{11/2}$ state via $^4F_{7/2}$ state. The ions of the excited $^2H_{11/2}$ state in a subsequent step relax to the ground state emitting green luminescence through ($^2H_{11/2}$, $^4S_{3/2}$) → $^4I_{15/2}$ transitions. Side by side a phenomenon of excited state cooperative energy transfer (ET) may also occur amongst the $^4I_{11/2}$—excited state Er^{3+} ions of the Er_2WO_6—nanocrystals

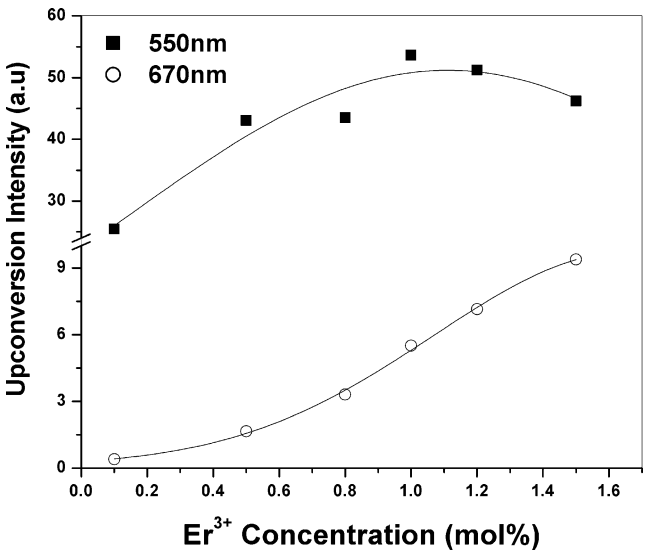

Fig. 8 Variation of upconversion intensity as a function of Er_2O_3 concentration

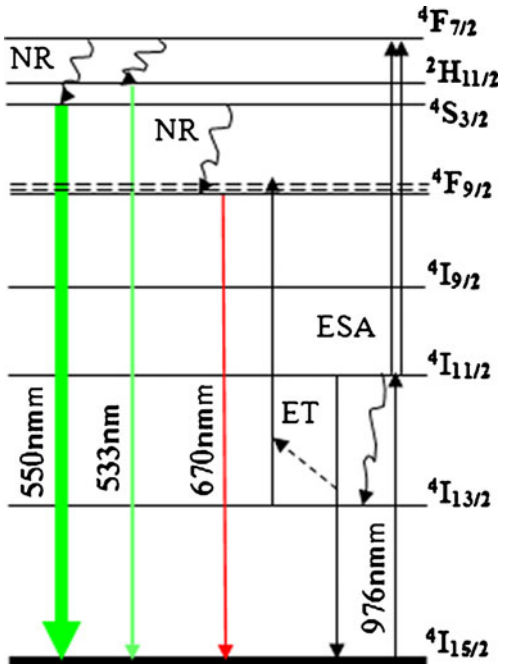

Fig. 9 Mechanism of green and red upconversion luminescence of Er^{3+} ions in the aged glass upon 976 nm NIR laser excitation

where Er^{3+} ions are at regular distance from each other. Thus the phenomenon of cooperative energy transfer (ET) further enhances the green luminescence efficiency of the Er^{3+} ions. As the laser power is increased, pumping of the ions to the excited $^4I_{11/2}$ state increases and hence the probability of both the excited state absorption (ESA) and the cooperative energy transfer (ET) increases and thereby, overall enhancement in the intensity of the green upconversion emission is observed. Such processes remain effective for the glasses containing Er^{3+} ions up to the concentration level of ~1 mol %. At concentration higher than 1 mol %, possibly the said processes reach a saturation limit and some other process starts, as evident from the observed greater increase in the red upconversion luminescence at the cost of green upconversion luminescence.

Let us now concentrate on the mechanism of red upconversion luminescence process of the aged glass. As mentioned above that the immediate low lying state of $^4I_{11/2}$ excited state is $^4I_{13/2}$. The life time of the $^4I_{13/2}$ state is also reasonably high (few milliseconds) [7, 15]. So a phenomenon of excited state absorption (ESA) of second 976 nm photons by the ions at the $^4I_{13/2}$ level may also be possible. Energy acquired by an Er^{3+} ion by this process however, takes the ion to a meta-stable phononic level lying in between $^4S_{3/2}$ and $^4F_{9/2}$ states. The ions therefore, subsequently cascade down to the $^4F_{9/2}$ state and then radiatively relax to the ground state through $^4F_{9/2} \rightarrow {}^4I_{15/2}$ transition creating red upconversion luminescence. At low concentration of Er^{3+}, the fraction of ions reaching the $^4I_{13/2}$ is relatively low; the intensity of the red emission therefore, remains low. As the Er^{3+} concentration in the glass is very much increased, the fraction of population of the ions in the $^4I_{13/2}$ state also increases and consequently the probability of energy transfer through cross relaxation between the ions of the excited $^4I_{11/2}$ and $^4I_{13/2}$ states $[(^4I_{11/2} + {}^4I_{13/2}) \rightarrow (^4I_{15/2} + {}^4F_{9/2})]$ increases and hence an overall enhancement of intensity of the red luminescence is obtained at the cost of the intensity of the green luminescence at higher concentration of Er^{3+}. Photo-physical path ways proposed respectively for the green and red upconversion luminescence are shown in Fig. 9.

Summary

The microscopic and nanoscopic structural properties of an Er^{3+} (1 mol %)—activated tungsten tellurite glass have been studied vis-à-vis the optical properties of its Er^{3+} ions, immediate after the preparation of the glass as well as after its ageing. It is noted that the glass suffers some structural reorganization in its network on ageing, which generates Er_2WO_6 nanocrystals in the matrix. The growth of Er_2WO_6 nanocrystals is found to greatly enhance both the normal and upconversion luminescence efficiency of Er^{3+} possibly because of different intra-centre excitation rates and/or different non-radiative decay path induced by the changed crystal field environment of Er^{3+} in the Er_2WO_6 nanocrystals. The material shows the prospect of use as good NIR solar concentrator.

Acknowledgement The corresponding author R. D. expresses his gratitude to CSIR, India, for grant-in-aid under Emeritus Scientist Scheme and the first author S.B. thanks the Director, CGCRI, Kolkata, for his encouragement.

References

1. Johnson LF, Guggenheim HJ (1971) Infrared-pumped visible laser. Appl Phys Lett 19(2):44–47
2. Kaminskii AA (1990) Laser crystals: their physics and properties, 2nd edn. Springer-Verlag, New York
3. Mori A, Ohishi Y, Sudo S (1997) Erbium doped tellurite glass fibre laser and amplifier. Electron Letts 33(10):863–864
4. Chen H, Liu YH, Zhou YF, Zhang QY, Jiang ZH (2005) Spectroscopic properties of Er^{3+} doped TeO_2-BaO (Li2O, Na_2O)–La_2O_3 glasses for 1.5 μm—optical amplifier. J Non-Cryst Solids 351(37–39):3060–3064
5. Hoyt CW, Sheik Bahae M, Epstein RI, Edwards BC, Anderson JE (2000) Observation of anti-stokes fluorescence cooling in thulium doped glasses. Phys Rev Letts 85:3600–3603
6. Martin IR, Velez P, Rodriguez VD, Rodriguez-Mendoza UR, Lavin V (1999) Upconversion dynamics in Er^{3+}-doped fluoroindate glasses. Spectrochimica Acta, Part-A 5:935–940
7. Lin H, Meredith G, Jiang S, Peng X, Luo T, Peghambarian N, Pun EY-B (2003) Optical transitions and visible upconversion in Er^{3+} doped niobic tellurite glass. J Appl Phys 93(1):186–192
8. Diaz-Torres LA, Dela Rossa-Cruz E, Salas P, Angeles Chavez C (2004) Concentration enhanced red upconversion in nanocrystalline ZrO_2: Er under IR excitation. J Phys D Appl Phys 37:2489–2495
9. Aebischer A, Heer S, Biner D, Kramer K, Haase M, Gudel HU (2005) Visible light emission upon near-infrared excitation in a transparent solution of nanocrystalline β-$NaGdF_4$:Yb^{3+}, Er^{3+}. Chem Phys Letts 407(1–3):124–128
10. Zeng J-H, Su J, Li Z-H, Yan R-X, Li Y-D (2005) Synthesis and upconversion luminescence of hexagonal-phase $NaYF_4$:Yb, Er^{3+} phosphors of controlled size and morphology. Advanced Mater 17:2119–2123
11. Sun H, Zhang L, Liao M, Zhou G, Yu C, Zhang J, Hu L, Jiang Z (2006) Host Dependent Frequency upconversion of Er^{3+}-doped oxyfluoride germanate glasses. J Lumin 117 (2):179–186
12. Vetrone F, Boyer JC, Capobianco JA, Speghini A, Bettinelli M (2002) 980 nm excited upconversion in an Er-doped ZnO-TeO_2 glass. Appl Phys Lett 80(10):1752–1754
13. Nayak A, Kundu P, Debnath R (2007) Strong green emission from Er^{3+} in a fluorine containing (Pb, La)-tellurite glass without using up-conversion route. J Non-Cryst Solids 353(13–15):1414–1417
14. Shalav A, Richards BS, Green MA (2007) Luminescent layers for enhanced silicon solar cell performance: Up-conversion. Solar Energy Mater Solar Cells 91(9):829–842
15. Ghosh A, Debnath R (2009) Enhanced electronic transition probabilities and line intensities of Er^{3+} ion in a (W, La)-tellurite

glass as revealed from Judd-Ofelt analysis. Sol Stat Commun 149 (25–26):1029–1032
16. Debnath R, Ghosh A, Balaji S (2009) Synthesis and luminescence properties of an ($Er_2Te_4O_{11}$) nanocrystals dispersed highly efficient lead free tellurite glass. Chem Phys Letts 474(4–6):331–335
17. Sokolov VO, Plotnichenko VG, Koltashev VV, Dianov EM (2006) On the structure of tungstate—tellurite glass. J Non-Cryst Solids 352(52–54):5618–5632
18. Van Oosternhout AB (1977) An ab initio calculation on the WO_6^{-6} octahedron with an application to its luminescence. J Chem Phys 67 (6):2412–2419
19. Blasse G, Dirkson GJ (1982) On the luminescence of rare-earth activated bismuth tungstates. J Sol Stat Chem 42(2):163–169
20. X-ray Data file No. 23-10701
21. Tyulin AV, Efremov VA, Trunov VK (1984) Crystal structure of orthorhombic (Er_2WO_6). Kristollografya 29(4):692–696
22. Tyulin AV, Efremov VA (1987) Polymorphism of oxytungstates La_2WO_6: Mechanism of structural transformations in Er_2WO_6. Kristollografya 32:363–370
23. Wang Z, Tong R, Lin H, Yang D (2009) Influence of WO_3 content on the optical properties of Eu^{3+}-doped Bi_2O_3–B_2O_3–WO_3 glasses. Mater Sci Poland 27(2):493–499